electronics

MDPI

Article

Design and Implementation of a Modular Multilevel Series-Parallel Converter for Second-Life Battery Energy Storage Systems

Esteban Concha [1], Ricardo Lizana F. [1,*], Sebastian Rivera [1,2] and Abraham M. Alcaide [3]

[1] Department of Electrical Engineering, Centro de Energia, Universidad Catolica de la Santisima Concepcion, Concepcion 4090541, Chile; econcha@ing.ucsc.cl (E.C.); s.rivera.i@ieee.org (S.R.)
[2] Department of Electrical Sustainable Energy, DCE&S Group, Delft University of Technology, 2628 CD Delft, The Netherlands
[3] Department of Electronic Engineering, University of Seville, 41004 Seville, Spain; amalcaide@us.es
* Correspondence: ricardolizana@ucsc.cl

Abstract: Battery Energy Storage Systems (BESS) offer scalable energy storage solutions, especially valuable for remote, off-grid applications. However, traditional battery packs with fixed series-parallel configurations lack reconfigurability and are limited by the weakest cell, hindering their application for second-life batteries. The Modular Multilevel Series-Parallel Converter (MMSPC) addresses these limitations by enabling dynamic reconfiguration, optimizing cell balancing, and enhancing energy control. This paper experimentally evaluates a single-phase BESS based on the MMSPC with an output power equivalent to 2 kW and two battery units (155V), demonstrating stable output and reduced internal losses across varied battery parameters.

Keywords: MMSPC; second-life batteries; energy storage

check for updates

Citation: Concha, E.; Lizana F., R.; Rivera, S.; Alcaide, A.M. Design and Implementation of a Modular Multilevel Series-Parallel Converter for Second-Life Battery Energy Storage Systems. *Electronics* **2024**, *13*, 4409. https://doi.org/10.3390/electronics13224409

Academic Editors: Luis M. Fernández-Ramírez, Jean-Christophe Crebier, Zhiwei Gao, Ahmed Abu-Siada, Kai Fu and Eladio Durán Aranda

Received: 2 October 2024
Revised: 30 October 2024
Accepted: 6 November 2024
Published: 11 November 2024

Copyright: © 2024 by the authors. Licensee MDPI, Basel, Switzerland. This article is an open access article distributed under the terms and conditions of the Creative Commons Attribution (CC BY) license (https://creativecommons.org/licenses/by/4.0/).

1. Introduction

Battery modules are based in the hard-wired connection of a large number of battery cells, aiming to achieve the desired voltage and current levels that each application requires. Typically, these cells are connected in series to reach a desired voltage, which are then connected in parallel to meet the current ratings. In off-grid application systems, there exists the need to secure the electrical energy results in several hundreds of cells permanently attached together [1]. This fixed series and parallel battery configuration is responsible for multiple difficulties, such as the need to continuously maintain the internal energy balance among the battery cells, along with the condition that the weakest cell determines the overall string performance [2,3]. There are different battery cell balancing methods, mainly classified as passive or active cell balancing. However, regardless of the selected cell balancing strategy, it will have limitations due to the power limits or aging of some cells [4,5]. This condition is especially critical if the battery pack is based on second life battery cells. This is due to the possibility that the battery cells come from different aging and applications, and that directly affects the possibility of achieving an internal voltage/power balance among the battery cells [5].

A solution to these difficulties is the integration of power electronics into the battery module, in order to enable a dynamic reconfiguration of the battery sub units (cells, modules, etc). This architecture is based on the power electronics building blocks (PEBB) paradigm, similar to the concept of modular converters, such as the Cascaded H-Bridge or the Modular Multilevel Converter, where the use of lower voltage units or cells is coordinated in such a way to achieve a higher voltage output [6]. In the case of a battery, the use of similar structures allow for the avoidance of a hard-wired connection of battery cells, leading to a highly flexible storage unit [7,8].

Consequently, within the power electronics units that can be integrated into the battery modules, the half or full H-bridge circuits appear as natural candidates. However,

in both configurations, the main difficulty is to guarantee a balance in the power among the battery units. Although some alternatives exist to alleviate such an imbalance, for instance, providing the MMC, or in delta-connected CHB, more degrees of freedom exist due to the circulating current control. However, this in turn reduces the efficiency of the system [5,9]. However, another power electronics structure that can further extend the benefits of conventional cells is the Modular Multilevel Series-Parallel Converter (MMSPC). The MMSPC provides important advantages compared with the traditional half or Full bridge power modules. The MMSPC not only allows for the series interconnection among them, but also allows their parallel interconnection. The parallel interconnection among the modules provides other features such as sensorless voltage balance (with no extra sensors or complex control/sorting algorithms). In addition, parallel connection also leads to a reduction in total parasitic inductance and resistance in the different energy paths. This is why the additional parallel state provided by the Modular Multilevel Series-Parallel Converter (MMSPC) is crucial for balancing the storage systems integrated into the power system, a feature that is absent in traditional Battery Energy Storage System (BESS) configurations [10,11].

The design of battery-based storage systems (BESS) based on the MMSPC allows the seamless integration of heterogeneous battery energy storage systems, and therefore the integration of second-cycle batteries as well. This converter allows the inherent voltage balance between the different battery modules with important advantages, since the entire system will not depend on the battery unit with the lowest quality or State of Health (SoH), which refers to the overall condition of the battery compared to when it was new, as well as the redundancy capacity of the system. In addition, this multilevel power converter presents a high-quality output voltage and current, which has an impact on the design of the passive output filtering stage, reducing its weight and size [12].

Other important aspects of a power converter are performance, efficiency, and reliability. These aspects have in common the power losses generated as well as the thermal stress undergone. In a multi-modular system, based on heterogeneous batteries, it is key that the balance between the batteries occurs intrinsically and that it also allows each power electronics module implemented in the topology to be subjected to an equivalent thermal stress. Since other multilevel converters present voltage stress mismatch (this is the case of CHB or other hybrids multilevel power converters), aging mismatch among the power modules or even within the power modules (this is the case of the popular MMC), the MMSPC converter allows for intrinsic power loss balancing and therefore equalized thermal stress, which results in a balanced Remaining Useful Lifetime (RUL) of the whole power converter [13]. By maintaining a homogeneous thermal stress in the modules, one of the factors that affects the useful life of semiconductors [14] is reduced. Finally, the acoustic noise that this system can generate is another interesting feature, since it is another aspect that can provide motivation to replace storage systems based on fossil fuels, which are noisy and generate polluting gases into the atmosphere during their operation. Instead, given the nature of the modulation strategy produced to generate the switching signals, the carrier frequency can be defined in order to reduce acoustic noise of the proposed system.

This paper presents a BESS based on the MMSPC converter with a simple energy balance operation among the battery units. In addition, this converter allows for the seamless combination of different battery modules as well as second-life batteries into a highly versatile and adaptable BESS. To ensure the stability and reliability of the system, a control strategy is proposed to maintain both the amplitude and frequency of the output voltage stable, independent of load impacts. The rest of the manuscript is distributed as follows: Section 2 explains the Topology used. Section 3 presents the control strategy as well as the pertinent modulation scheme. Section 4 illustrates the feasibility of the proposal in the down-scaled experimental mock-up. Finally, in Section 5, the conclusions of the work are presented.

2. Topology Description

The BESS based on the use of the MMSPC converter topology is presented in Figure 1. A generalized version of the structure is displayed in Figure 1a, showing the capability of integrating several types of battery modules with reconfigurable capability by the means of power electronics cells. This reconfigurable structure is not only beneficial for using heterogeneous battery modules, since it also features a high-quality output given its multilevel behavior [15]. A single-phase version is chosen for the sake of simplicity and to allow for a direct comparison with a diesel generator in residential applications, as displayed in Figure 1b. This comparison is due to the fact that diesel generators are actually the traditional and accessible way to generate electricity in sectors that do not have access to the conventional electric grid. However, these generators use fossil fuels that generate air pollution, as well as generating considerable noise. For this reason, it is necessary to look for alternatives that allow operation and generation of electricity in remote sectors and that are environmentally sustainable, and do not need a complicated or sophisticated control scheme. Moreover, it is important to highlight the fact that the presented approach can be directly extended to three-phase systems, for industrial applications that require higher power levels.

This BESS structure is composed by three different parts: a distributed battery solution integrated in the MMSPC cells, an output filter stage based on the conventional LCL filter structure and a resistive load.

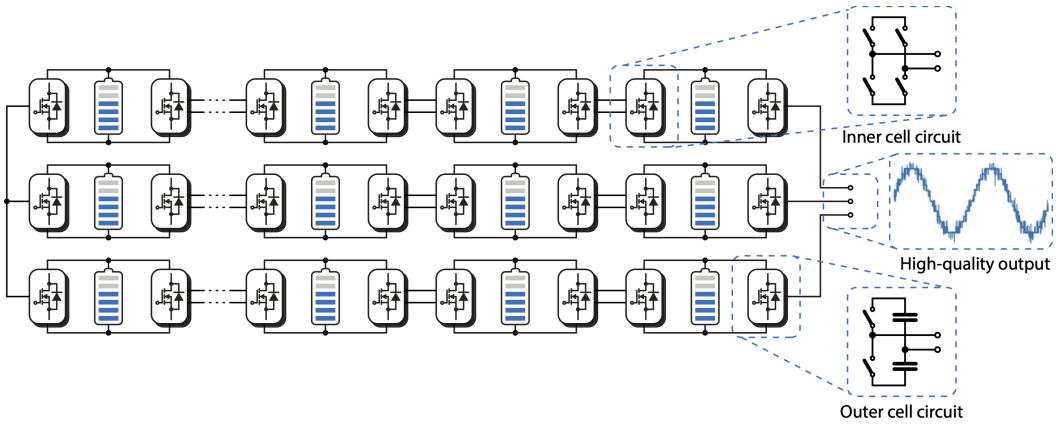

Figure 1. Battery energy storage system (BESS) based on the modular multilevel series-parallel converter topology in grid-forming applications. (**a**) Generalized multicell three-phase structure for a reconfigurable BESS. (**b**) Single-phase approach considering an LCL filtering stage and two cells.

The basic structure of the Modular Multilevel Series-Parallel Converter (MMSPC) is based on multiple power cells (n) connected in series, similar to a Cascaded H-Bridge (CHB) topology. Each cell comprises eight semiconductors along with a storage unit. These eight semiconductors are configured to enable series, bypass, or parallel connections among the power cells. This latter configuration, which represents an additional degree of freedom provided by MMSPC cells compared to traditional modules like the H-Bridge, enables balancing across the interconnected storage units in the system [16,17]. The decision regarding

when to activate this additional parallel connection mode is delegated to the modulation stage. Various modulation strategies have emerged, aiming to optimize the internal balancing of the storage units as well as to reduce the system's internal losses [15,18–20].

As shown in Figure 1, the MMSPC converter is composed by $n = 2$ cells for its experimental validation. However, it is important to highlight that the system is completely modular and scalable. This is because voltage and power levels can be adjusted by increasing or decreasing the number of cells n connected within the proposed system. The key feature of the MMSPC modules is the capacity to enable the internal balance among the storage units without extra requirements or complex control and/or modulation algorithms or the use of external or additional sensors [12,17,21].

The modulation strategy implemented is based on the PS-PWM method and has already been published in previous works [18]. The main objective is to maximize the number of times that the modules are connected in parallel, but only for short periods. In this way, the internal balance between the storage systems can be regulated through the frequency of the triangular carrier. The modulation strategy allows for the generation of the states that connect the battery modules in series, parallel or bypass, leading to a simple and sensorless balanced operation of the batteries. The method of selecting the switching states basically depends on whether the switching of the internal or the external interconnections between the modules is being controlled. In general terms, the modulation is based on a Phase-Shifter PWM modulation strategy, where the switching states selected by the modulation strategy are defined by the interconnection between two modules. Using this concept, it is possible to define two types of interconnections: The internal interconnections which are focused in the interconnection between two adjacent modules (from Figure 1 are S_3,S_4,S_5 and S_6), and the external interconnection, which refers to the switches located at both ends of the converter (from Figure 1 are S_1,S_2,S_7 and S_8). The carriers are implemented with a phase-shift angle defined by

$$\theta = \frac{\pi}{n} \tag{1}$$

Since the system is validated with $n = 2$, it is necessary to define two couples of carrier signals. For the internal interconnections of the system, one triangular carrier and its polarity inverter signal are employed (C_1 and C_{1N}), as is described in Figure 2. If the modulation signal is greater than the triangular carriers C_1 and C_{1N}, a series positive state is selected (Figure 2c). If the modulation signal is smaller than the triangular carriers, a series negative state is selected (Figure 2d), otherwise a parallel connection between the modules is implemented (Figure 2a). On the other hand, for the external interconnection, the modulation strategy alternates between series and bypass connections, as displayed in Figure 3. The idea of the selection states is basically the comparison among the modulation signal and the carriers C_2 and C_{2N}. The difference with the internal interconnection is that the parallel interconnection is replaced by a bypass interconnection, as is presented in Figure 3.

There are many methods for the design of the LCL filter stage [22]. In this work, for the sake of simplicity, for the design of the third-order LCL output filter, the guidelines from [23,24] are adjusted for a multilevel single-phase inverter enabled by a battery array. First, the battery is sized in such a way that at the lowest state of charge (SoC), the amplitude modulation index remains above 0.95 to ensure the converter can maintain a steady output voltage under any scenario. Then, the first inductive stage of the filter L_1 will be designed to keep the converter-side current with a ripple under 5% at the worst operating condition. Additionally, the filter capacitance C_f is limited to absorb 4% of reactive power during rated power operation. Finally, the grid-side inductance L_2 is selected in such a way that the voltage drop across both reactors is below 5% at the rated power operation, while locating the resonant frequency of the filter in the range $[10F_o, 0.5F_{sw}]$ [23,24]. These conditions lead to

$$C_f = 0.04C_b \tag{2}$$

$$L_1 + L_2 \leq 0.05L_b \tag{3}$$

$$L_1 = \frac{3 \cdot n \cdot V_{dc}}{4F_{sw}\Delta I_{o_{\max}}}(1 - m_a) \tag{4}$$

where C_b is the base capacitance of the system, L_b is the base inductance, n is the number of modules per phase of the MMSPC, $\Delta I_{o_{\max}}$ is the maximum current ripple at the converter side at rated power, V_{dc} is the DC voltage of the battery modules and F_{sw} the output equivalent switching frequency.

$$L_2 = \frac{L_1}{\omega_{res}^2 L_1 C_f - 1} \tag{5}$$

where ω_{res} is the resonance frequency of the LC filter. The experimental parameters for the LCL is presented in the Table 1.

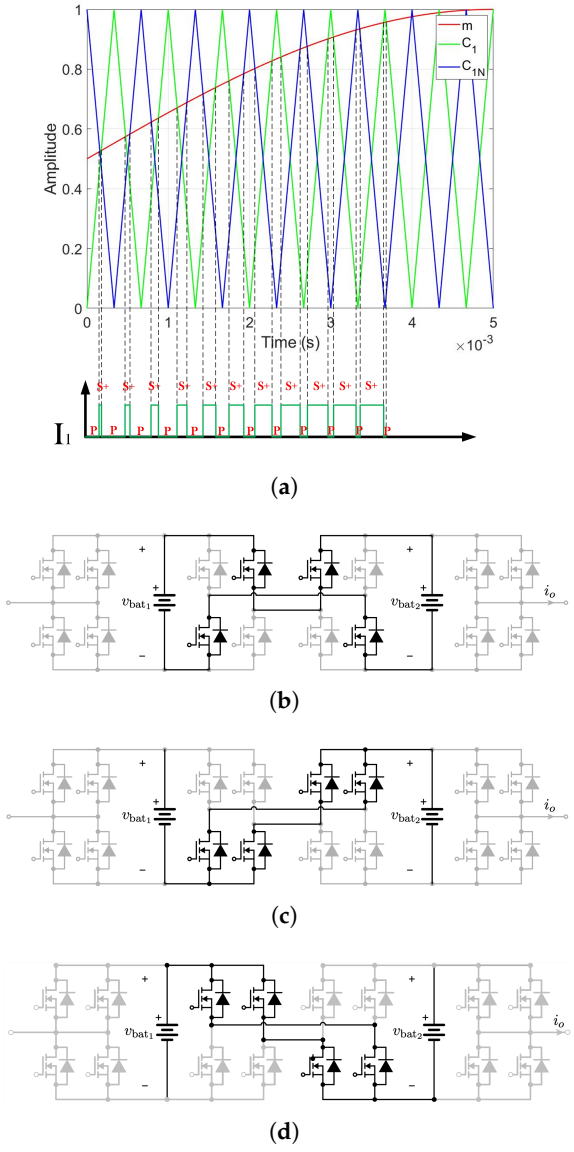

Figure 2. Modulation strategy for internal interconnection modules. (**a**) Triangular carrier definition and pulses generation. (**b**) Module parallel connection. (**c**) Module serial positive connection. (**d**) Module serial negative connection.

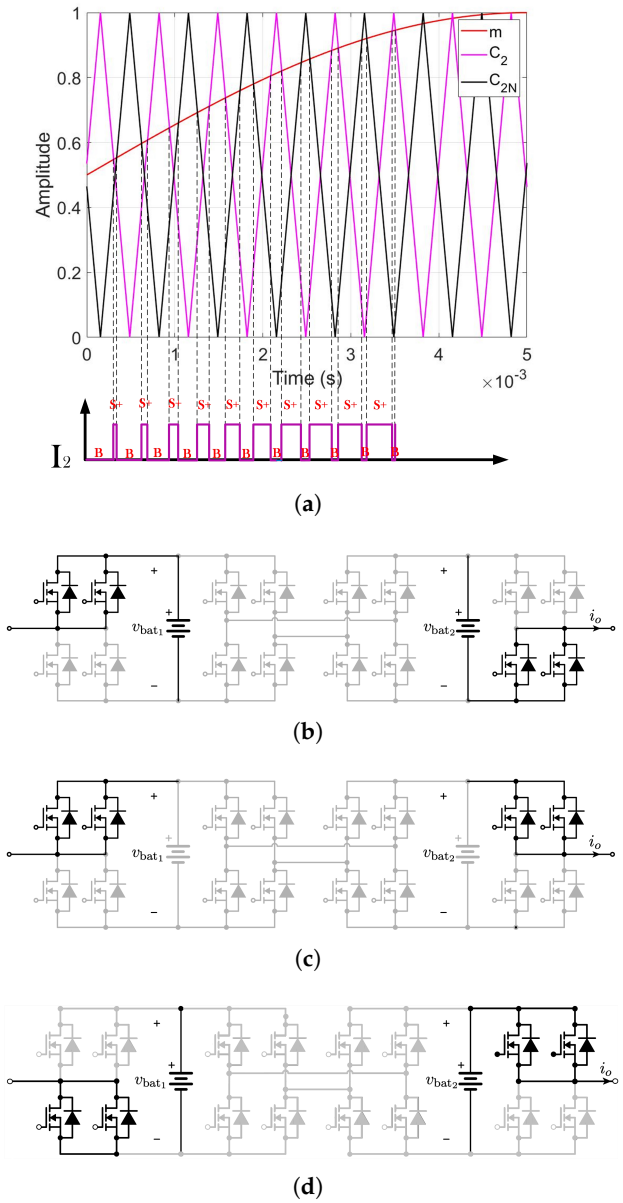

Figure 3. Modulation strategy for external interconnection modules. (**a**) Triangular carrier definition and pulses generation. (**b**) Serial positive connection. (**c**) Bypass connection. (**d**) Serial negative connection.

Table 1. Simulation and Experimental Parameters.

Parameter	Simulation Values	Experimental Values
Battery voltage v_{bat_1}, v_{bat_2}	155 V	155 V
Carrier frequency of modulation framework	3 kHz	3 kHz
Filter Inductance L_1	1.1 mH	1.1 mH
Filter Inductance L_2	1.2 mH	1.2 mH
Filter Capacitance C_f	21.37 µF	25 µF
Load Resistance R	200 Ω	200 Ω
Resonance frequency	1.45 kHz	1.34 kHz
AC output frequency	50 Hz	50 Hz

3. Control Strategy

The control strategy displayed in Figure 4 allows for the precise regulation of the AC output voltage amplitude and frequency, regardless of the load condition in the system. This aspect is fundamental for the application of BESS systems operating in grid-forming mode. Moreover, as discussed in Section 2, the modulation strategy guarantees the voltage balance among the batteries. This fact is critical to maintain the power quality of multilevel converters and reduce the total harmonic distortion (THD) of the output voltage/current signals. To achieve this, the system output voltage is sensed and compared to a reference voltage. The control stage is performed via a cascaded control loop. The result of this control scheme is the modulation signal, and it feeds into the modulation strategy.

The parameters for the PI controllers were obtained from the equations described in (6) and (7), and detailed in the Table 2.

$$\frac{v_o}{i_o} = \frac{1}{\frac{C_f \cdot L_2 \cdot s^2}{R} + C_f \cdot s + \frac{1}{R}} \tag{6}$$

$$\frac{i_o}{m_a} = \frac{1}{L_1 \cdot s + R_1} \tag{7}$$

Table 2. PI controller parameters.

Controller	Proportional Gain	Integration Gain
Current Controller	$k_{pi} = -0.0085$	$k_{Ti} = 0.00023$
Voltage Controller	$k_{pv} = 0.14$	$k_{Tv} = 0.0045$

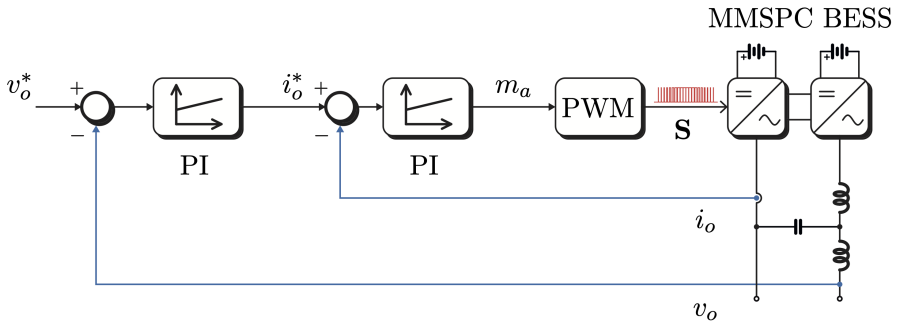

Figure 4. Control strategy.

4. Experimental Results

A small-scale BESS has been developed for laboratory testing. The proper operation and balancing capabilities of the proposal are validated using a the setup shown in Figure 5, where it is possible to identify the MMSPC converter, LCL filter, battery emulator and the load. The scenarios that will be analyzed in the experimental platform include: dynamic performance under a 100% load impact, balancing of different SoCs among the units, balancing current analysis during parallel states and thermal analysis of the setup.

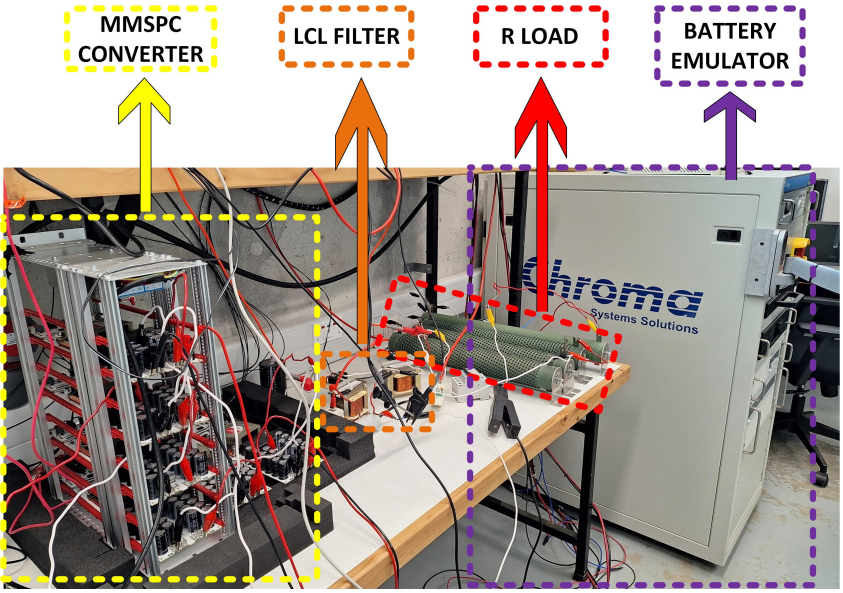

Figure 5. Experimental setup.

4.1. Load Impact

For the first case study, it is proposed that both batteries connected to the converter have the same SoC. The experiment begins with a no-load system, followed by a 200 Ω load impact with the objective of verifying the stability of the system and its ability to stabilize the batteries' energy without the need for dedicated sensors or control loops. The results of this experiment are shown in Figure 6. It is important to note that during this process, the converter voltage remains totally stable not only in the power converter terminals but also in the output LCL filter stage reaching a voltage peak of 311 V with a voltage frequency equal to 50 Hz, as is shown in Figure 6a. The resulting load current increases from 0 A to approximately 1.5 A, as shown in Figure 6b.

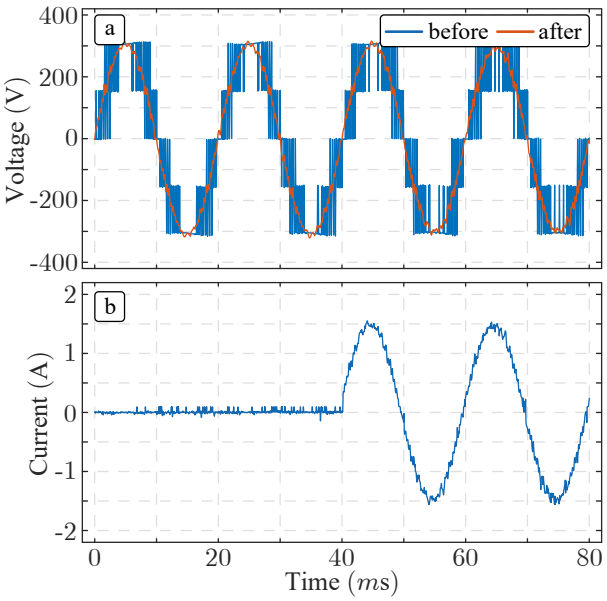

Figure 6. Experimental results for load impact verification. (**a**) Output voltage of the MMSPC converter during the load insertion in its terminals (blue) and in the LCL output filter (red). (**b**) Resulting transient current after a load insertion.

In addition, upon analyzing Figure 7, which represents the SOC and voltages of both batteries, it can be observed that after the load impact, they tend to stabilize at the

same voltage and SOC value. This validates the earlier statement regarding the inherent stabilization of the energy storage elements connected to the converter, facilitated by the serial and parallel connections achievable with the MMSPC topology.

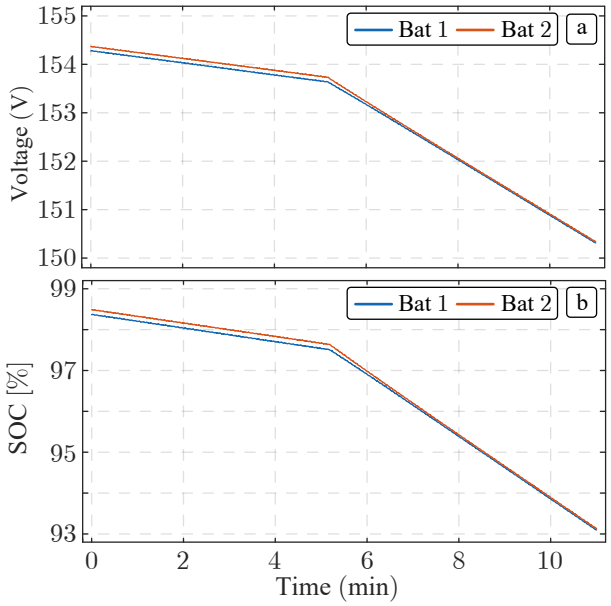

Figure 7. Evolution of the battery quantities during the load impact experiment. (**a**) Voltage measurements in modules 1 (blue) and 2 (red). (**b**) State of Charge in modules 1 (blue) and 2 (red).

4.2. Battery Energy Balance

On the other hand, a second case study was conducted where the batteries had a 3% difference in their SoC. In this scenario, the same load was connected from the beginning and the results are shown in Figure 8. As is shown in Figure 8a, the resulting power converter output voltage does not present any unbalance despite of the battery voltage unbalance. This fact demonstrates the high quality output current in the connected load, as is shown in Figure 8b.

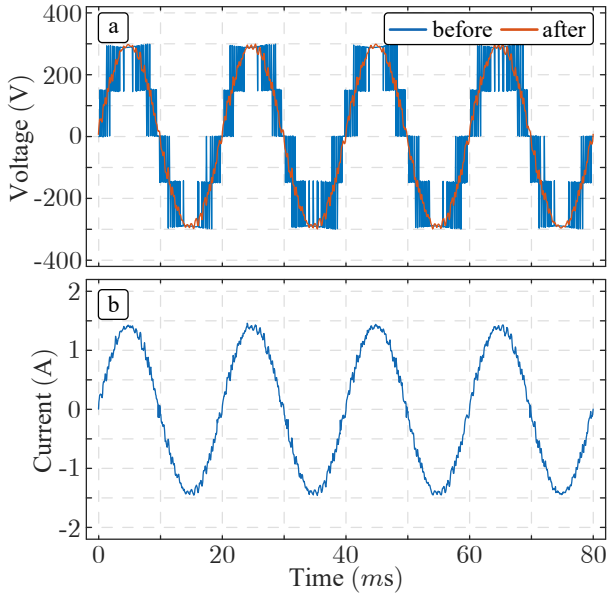

Figure 8. Experimental results for battery energy balance verification. (**a**) Output voltage of the MMSPC converter during the load insertion in its terminals (blue) and in the LCL output filter (red). (**b**) Resulting transient current during energy balance.

The MMSPC converter allows for the achievement of the balance between the heterogeneous batteries connected to the system, appreciating the effect of the balance dynamics in Figure 9 referring to the voltage and SoC, validating the capacity of the system-based MMSPC to achieve an internal balance between energy storage units.

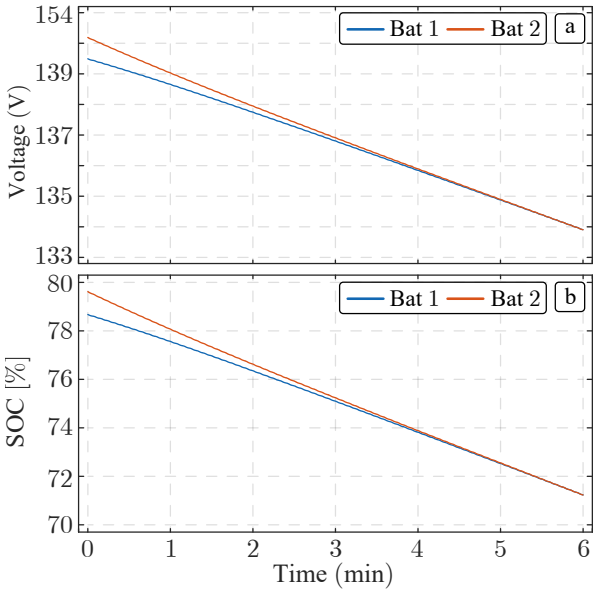

Figure 9. Evolution of the battery quantities during the energy balance experiment. (**a**) Voltage measurements in modules 1 (blue) and 2 (red). (**b**) State of Charge in modules 1 (blue) and 2 (red).

It is important to highlight that the balance between the batteries integrated into the system is executed and developed decoupled from the control of the current and voltage connected to the load.

4.3. Parallelization Current Analysis

As previously mentioned, internal currents in the MMSPC depend on the parallel interconnection periods. In this sense, the effective switching frequency forced by the carrier frequency adopts a key factor. Higher switching frequencies limit the internal current peaks but also increase the switching loss of the whole power converter. On the contrary, reducing switching frequency helps to reduce the switching loss but the internal current peaks could be very high. This phenomenon is clearly shown in Figure 10a.

In order to mitigate the internal current surges, the integration of an inductance among modules can also be considered, in order to dampen the dynamics of the currents, especially in cases where the batteries interconnected in the system have considerable voltage differences. This effect is shown in Figure 10b where a 5 mH inductance in the interconnection between the modules has been integrated.

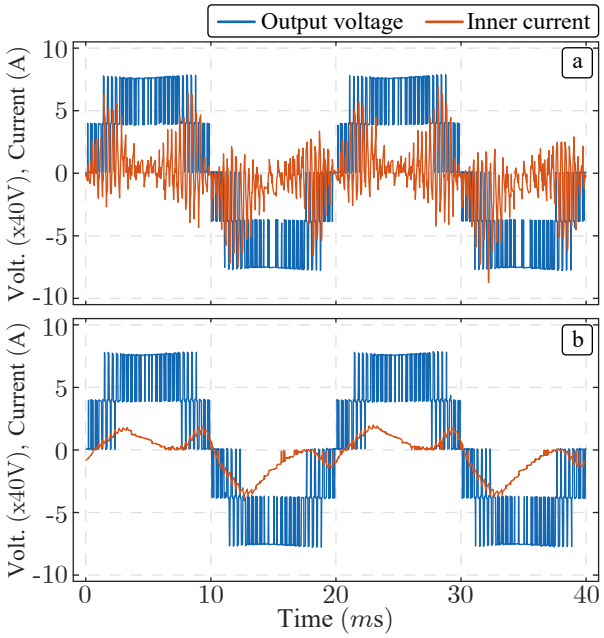

Figure 10. Comparative of the Internal Current between modules and output voltage of the converter. (**a**) Without inductor. (**b**) Using an interconnection inductor .

4.4. Thermal Losses in Power Modules

Figure 11 shows a thermal photograph presenting the maximum and minimum heat points observed in the MOSFET modules. In this figure, seven measurements were carried out: one before starting to operate the converter and the other six with an interval of 10 min between each sample, until completing 60 min. In this way, it was observed that the modules maintain a similar temperature to each other, presenting slight variations, and maintain an average temperature of 38 °C, with local maximums of up to 45 °C. These maxima are represented in the figure as points in the deep red module. With these results, it is confirmed that not only the voltages of the batteries connected to the converter are balanced, but also that the converter losses are distributed uniformly. However, one of the modules exceeds the average values presented in Table 3, reaching maxima of up to 51.4 °C. This is because this module was powered with a different DC source than the one provided by default by the company that develop the power modules.

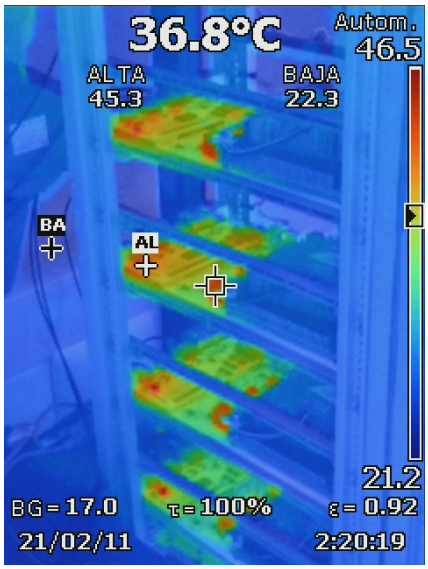

Figure 11. Thermography of the modules.

Table 3. Temperature measurements.

Time	Temperature
0 min	24.0 °C
10 min	31.9–44.8 °C
20 min	33.5–42.8 °C
30 min	32.0–43.5 °C
40 min	31.8–43.8 °C
50 min	36.8–45.3 °C
60 min	37.2–43.8 °C

5. Conclusions

In this work, we presented a Second Life BESS based on a MMSPC configuration. The proposed topology effectively demonstrates the ability to implement an electric power generation system utilizing batteries while ensuring high-quality voltage waveforms due to its multilevel architecture. Additionally, this configuration inherently balances the battery units, enabling the integration of second-life batteries without compromising the system's dynamics and operational integrity.

However, a significant limitation identified in the proposed system is the variability among the battery modules. When the voltage and dynamic characteristics of the second-life batteries differ substantially, the integration of coupling inductances between the modules becomes essential to mitigate potential current peaks, thereby preserving the overall system efficiency. Moreover, the analysis indicates that operational losses are distributed across the various modules, reinforcing the viability of the proposed solution as an environmentally sustainable energy backup system.

Future research should explore strategies for optimizing the integration of heterogeneous battery technologies and advanced control methodologies to further enhance system performance and reliability.

Author Contributions: Investigation, E.C., R.L.F., S.R. and A.M.A.; Writing—original draft, E.C., R.L.F., S.R. and A.M.A.; Writing—review & editing, E.C., R.L.F., S.R. and A.M.A. All authors have read and agreed to the published version of the manuscript.

Funding: This research was funded by the Chilean National Agency for Research and Development (ANID) through the grants: FONDECYT Regular no. 1230306; Beca Santander Investigadores: 2021; AC3E ANID/BASAL/AFB240002; FAA-UCSC: 2023; Centro de Energía UCSC: 2024; SERC Chile: ANID/FONDAP/1522A0006.

Data Availability Statement: The raw data supporting the conclusions of this article will be made available by the authors on request.

Conflicts of Interest: The authors declare no conflicts of interest.

References

1. Leon, J.I.; Dominguez, E.; Wu, L.; Marquez Alcaide, A.; Reyes, M.; Liu, J. Hybrid Energy Storage Systems: Concepts, Advantages, and Applications. *IEEE Ind. Electron. Mag.* **2021**, *15*, 74–88. [CrossRef]
2. Shahjalal, M.; Shams, T.; Islam, M.E.; Alam, W.; Modak, M.; Hossain, S.B.; Ramadesigan, V.; Ahmed, M.R.; Ahmed, H.; Iqbal, A. A review of thermal management for Li-ion batteries: Prospects, challenges, and issues. *J. Energy Storage* **2021**, *39*, 102518. [CrossRef]
3. Cai, H.; Liu, X.; Sun, L.; Xu, Y.; Wang, Y.; Han, X.; Zheng, Y.; Sun, Y.; Ouyang, M. Battery internal short circuit diagnosis based on vision transformer without real data. *Innov. Energy* **2024**, *1*, 100041. [CrossRef]
4. Lelie, M.; Braun, T.; Knips, M.; Nordmann, H.; Ringbeck, F.; Zappen, H.; Sauer, D.U. Battery Management System Hardware Concepts: An Overview. *Appl. Sci.* **2018**, *8*, 534. [CrossRef]
5. Poblete, P.; Cuzmar, R.H.; Aguilera, R.P.; Pereda, J.; Alcaide, A.M.; Lu, D.; Siwakoti, Y.P.; Konstantinou, G. Dual-Stage MPC for SoC Balancing in Second-Life Battery Energy Storage Systems Based on Delta-Connected Cascaded H-Bridge Converters. *IEEE Trans. Power Electron.* **2024**, 1–16. [CrossRef]
6. Restrepo, C.; González-Castaño, C.; Giral, R. The Versatile Buck-Boost Converter as Power Electronics Building Block: Changes, Techniques, and Applications. *IEEE Ind. Electron. Mag.* **2023**, *17*, 36–45. [CrossRef]

7. Huang, Y.; Liu, F.; Zhuang, Y.; Diao, X.; Lei, Y.; Zhu, H. Bidirectional Three-Port Converter for Modular Multilevel Converter-Based Retired Battery Energy Storage Systems. *IEEE Trans. Power Electron.* **2024**, *39*, 11148–11163. [CrossRef]
8. He, R.; Tian, K.; Ling, Z. Offline Equalization Control of Modular Multilevel Converter-Based Battery Energy Storage System. *IEEE Trans. Ind. Electron.* **2024**, *71*, 9003–9012. [CrossRef]
9. Zhang, L.; Qin, J.; Zou, Y.; Duan, Q.; Sheng, W. Analysis of Capacitor Charging Characteristics and Low-Frequency Ripple Mitigation by Two New Voltage-Balancing Strategies for MMC-Based Solid-State Transformers. *IEEE Trans. Power Electron.* **2021**, *36*, 1004–1017. [CrossRef]
10. Helling, F.; Götz, S.; Singer, A.; Weyh, T. Fast Modular Multilevel series/Parallel Converter for direct-drive gas turbines. In Proceedings of the 2015 IEEE NW Russia Young Researchers in Electrical and Electronic Engineering Conference (EIConRusNW), St. Petersburg, Russia, 2–4 February 2015; pp. 198–202. [CrossRef]
11. Wang, C.; Li, Z.; Murphy, D.L.K.; Li, Z.; Peterchev, A.V.; Goetz, S.M. Photovoltaic Multilevel Inverter with Distributed Maximum Power Point Tracking and Dynamic Circuit Reconfiguration. In Proceedings of the 2017 IEEE 3rd International Future Energy Electronics Conference and ECCE Asia (IFEEC 2017—ECCE Asia), Kaohsiung, Taiwan, 3–7 June 2017; pp. 1520–1525. [CrossRef]
12. Bahamonde I., H.; Rivera, S.; Li, Z.; Goetz, S.; Peterchev, A.; Lizana F., R. Different parallel connections generated by the Modular Multilevel Series/Parallel Converter: An overview. In Proceedings of the IECON 2019—45th Annual Conference of the IEEE Industrial Electronics Society, Lisbon, Portugal, 14–17 October 2019; Volume 1, pp. 6114–6119. [CrossRef]
13. Zhang, J.; Tian, J.; Alcaide, A.M.; Leon, J.I.; Vazquez, S.; Franquelo, L.G.; Luo, H.; Yin, S. Lifetime Extension Approach Based on the Levenberg–Marquardt Neural Network and Power Routing of DC–DC Converters. *IEEE Trans. Power Electron.* **2023**, *38*, 10280–10291. [CrossRef]
14. Kuprat, J.; van der Broeck, C.H.; Andresen, M.; Kalker, S.; Liserre, M.; De Doncker, R.W. Research on Active Thermal Control: Actual Status and Future Trends. *IEEE J. Emerg. Sel. Top. Power Electron.* **2021**, *9*, 6494–6506. [CrossRef]
15. Goetz, S.M.; Li, Z.; Peterchev, A.V.; Liang, X.; Zhang, C.; Lukic, S.M. Sensorless scheduling of the modular multilevel series-parallel converter: Enabling a flexible, efficient, modular battery. In Proceedings of the 2016 IEEE Applied Power Electronics Conference and Exposition (APEC), Long Beach, CA, USA, 20–24 March 2016; pp. 2349–2354. [CrossRef]
16. Korte, C.; Specht, E.; Hiller, M.; Goetz, S. Efficiency evaluation of MMSPC/CHB topologies for automotive applications. In Proceedings of the 2017 IEEE 12th International Conference on Power Electronics and Drive Systems (PEDS), Honolulu, HI, USA, 12–15 December 2017; pp. 324–330. [CrossRef]
17. Goetz, S.M.; Li, Z.; Liang, X.; Zhang, C.; Lukic, S.M.; Peterchev, A.V. Control of Modular Multilevel Converter with Parallel Connectivity—Application to Battery Systems. *IEEE Trans. Power Electron.* **2017**, *32*, 8381–8392. [CrossRef]
18. Tashakor, N.; Iraji, F.; Goetz, S.M. Low-Frequency Scheduler for Optimal Conduction Loss in Series/Parallel Modular Multilevel Converters. *IEEE Trans. Power Electron.* **2022**, *37*, 2551–2561. [CrossRef]
19. Tashakor, N.; Arabsalmanabadi, B.; Cervera, L.O.; Hosseini, E.; Al-Haddad, K.; Goetz, S. A Simplified Analysis of Equivalent Resistance in Modular Multilevel Converters with Parallel Functionality. In Proceedings of the IECON 2020 The 46th Annual Conference of the IEEE Industrial Electronics Society, Singapore, 18–21 October 2020; pp. 4158–4163. [CrossRef]
20. Fang, J.; Li, Z.; Goetz, S.M. Multilevel Converters with Symmetrical Half-Bridge Submodules and Sensorless Voltage Balance. *IEEE Trans. Power Electron.* **2021**, *36*, 447–458. [CrossRef]
21. Goetz, S.M.; Peterchev, A.V.; Weyh, T. Modular Multilevel Converter with Series and Parallel Module Connectivity: Topology and Control. *IEEE Trans. Power Electron.* **2015**, *30*, 203–215. [CrossRef]
22. Gao, C.; He, S.; Kong, R.; Leung, K.N.; Loh, P.C. Passivity-Based Controller Design of LCL-Filtered Selective-Harmonic Resistive-Active Power Filter. *IEEE Trans. Ind. Electron.* **2024**, 1–11. [CrossRef]
23. Liserre, M.; Blaabjerg, F.; Hansen, S. Design and control of an LCL-filter-based three-phase active rectifier. *IEEE Trans. Ind. Appl.* **2005**, *41*, 1281–1291. [CrossRef]
24. Reznik, A.; Simões, M.G.; Al-Durra, A.; Muyeen, S.M. *LCL* Filter Design and Performance Analysis for Grid-Interconnected Systems. *IEEE Trans. Ind. Appl.* **2014**, *50*, 1225–1232. [CrossRef]

Disclaimer/Publisher's Note: The statements, opinions and data contained in all publications are solely those of the individual author(s) and contributor(s) and not of MDPI and/or the editor(s). MDPI and/or the editor(s) disclaim responsibility for any injury to people or property resulting from any ideas, methods, instructions or products referred to in the content.